

Synthesis and Processing of Monodisperse Oligo(fluorene-co-bithiophene)s into Oriented Films by Thermal and Solvent Annealing

By Lichang Zeng, Feng Yan, Simon K.-H. Wei, Sean W. Culligan, and Shaw H. Chen*

A series of oligo(fluorene-co-bithiophene)s, OF2Ts, have been synthesized and characterized to investigate the effects of oligomer length and pendant aliphatic structure on glassy-nematic mesomorphism. The OF2Ts comprising more than one repeat unit and their polymer analogue, PF2T, carrying 52 number-average repeat units, possess the highest occupied molecular orbital energy level at -5.3 ± 0.2 eV, but the anisotropic field-effect mobilities increase with the oligomer length. Spin coating from high-boiling chlorobenzene with and without subsequent exposure to saturated chlorobenzene vapor constitute solvent-vapor annealing and quasi-solvent annealing, respectively. Solvent-vapor annealing yields monodomain glassy-nematic films in which OF2Ts are aligned as well as with thermal annealing across a 2 cm diameter. Quasi-solvent annealing, however, amounts to kinetically trapping a lower orientational order than solvent-vapor or thermal annealing. While amenable to thermal annealing at elevated temperatures, PF2T shows no alignment at all following either strategy of solvent annealing.

conjugated backbones offers additional desirable features, such as polarized light emission to obviate polarizers in liquid crystal displays and anisotropic charge transport to suppress cross-talk in logic circuit and pixel switching elements. Numerous backbone alignment strategies have been demonstrated for liquid crystalline poly(9,9'-dioctylfluorene),^[12–20] PF, and poly(9,9'-dioctylfluorene-co-bithiophene),^[21–25] PF2T, including rubbed polymer films,^[12–14,19,21] photoalignment induced by polarized irradiation,^[15,25] and friction transfer.^[16,19,22] In addition to liquid crystallinity, both PF and PF2T are capable of preserving polymer backbone alignment in the solid state through glass transition. The hole mobility along the uniaxially aligned PF2T film has been reported to be 10 times that of the perpendicular component and about 3 times that observed in an isotropic film.^[21] For a facile hole injection from gold

1. Introduction

Organic materials with an extended π -conjugation have found numerous potential applications to electronics and photonics,^[1–5] most notably in light-emitting diodes, field-effect transistors, and solar cells. Conjugated polymers can be prepared into thin films through solution processing across a large area, thus offering a cost advantage over small molecules that are typically deposited by vacuum sublimation. As an integral part of flexible electronics, polymer-based organic field-effect transistors have been actively pursued over the past decade, generating a wealth of information on charge-carrier mobility as a function of polymer morphology, gate insulator, and device architecture.^[6–11] Uniaxial alignment of

with a Fermi level at -5.2 eV, PF2T is better suited for field-effect transistors than PF in terms of the highest occupied molecular orbital (HOMO) energy level, -5.5 versus -5.8 eV.^[14,26] Regioregular poly(3-hexylthiophene) is superior to PF and PF2T in terms of hole mobility on the order of $0.1 \text{ cm}^2 \text{ V}^{-1} \text{ s}^{-1}$ ^[27,28] and ease of hole injection (with a HOMO level at -4.9 eV) from gold, but is inferior in oxidative stability as with polythiophenes in general.^[29] With somewhat improved oxidative stability because of the lower HOMO level of -5.1 eV, thermotropic liquid crystalline thieno[3,2-*b*]thiophene polymers have been reported with a hole mobility of $0.2\text{--}0.6 \text{ cm}^2 \text{ V}^{-1} \text{ s}^{-1}$ in crystalline domains.^[30]

Normally synthesized by step-growth polymerization, π -conjugated polymers are characterized by distributed chain lengths. The divergent-convergent approach to the synthesis of conjugated oligomers^[31–33] offers monodisperse molecular systems readily soluble in benign organic solvents to facilitate purification by recrystallization, column chromatography, or vacuum sublimation. Compared to polydisperse conjugated polymers with a high molecular weight, monodisperse conjugated oligomers are more amenable to structural optimization for thermotropic properties, such as the type of mesomorphism as well as glass-transition and clearing temperatures. In the absence of chain entanglements and defects, relatively short and uniform chains are also conducive to the formation of monodomain films by monodisperse conjugated

[*] Prof. S. H. Chen, L. C. Zeng, F. Yan, S. K.-H. Wei, S. W. Culligan
Department of Chemical Engineering
University of Rochester
Rochester, NY 14627-0166 (USA)
E-mail: shch@lle.rochester.edu
Prof. S. H. Chen
Laboratory for Laser Energetics
250 East River Road
University of Rochester
Rochester, NY 14623-1212 (USA)

DOI: 10.1002/adfm.200900101

oligomers. To take advantage of these favorable material traits, a number of monodisperse oligo(fluorene)s,^[31–40] OFs, and oligo(fluorene-co-bithiophene)s,^[41–43] OF2Ts, have been reported, but challenges remain in the understanding of how molecular structures affect material properties that are critical to the performance of polarized light-emitting diodes and anisotropic field-effect transistors. Of particular interest is the ability of conjugated oligomers to form glassy liquid crystalline films with elevated phase transition temperatures and superior stability against thermally activated crystallization.

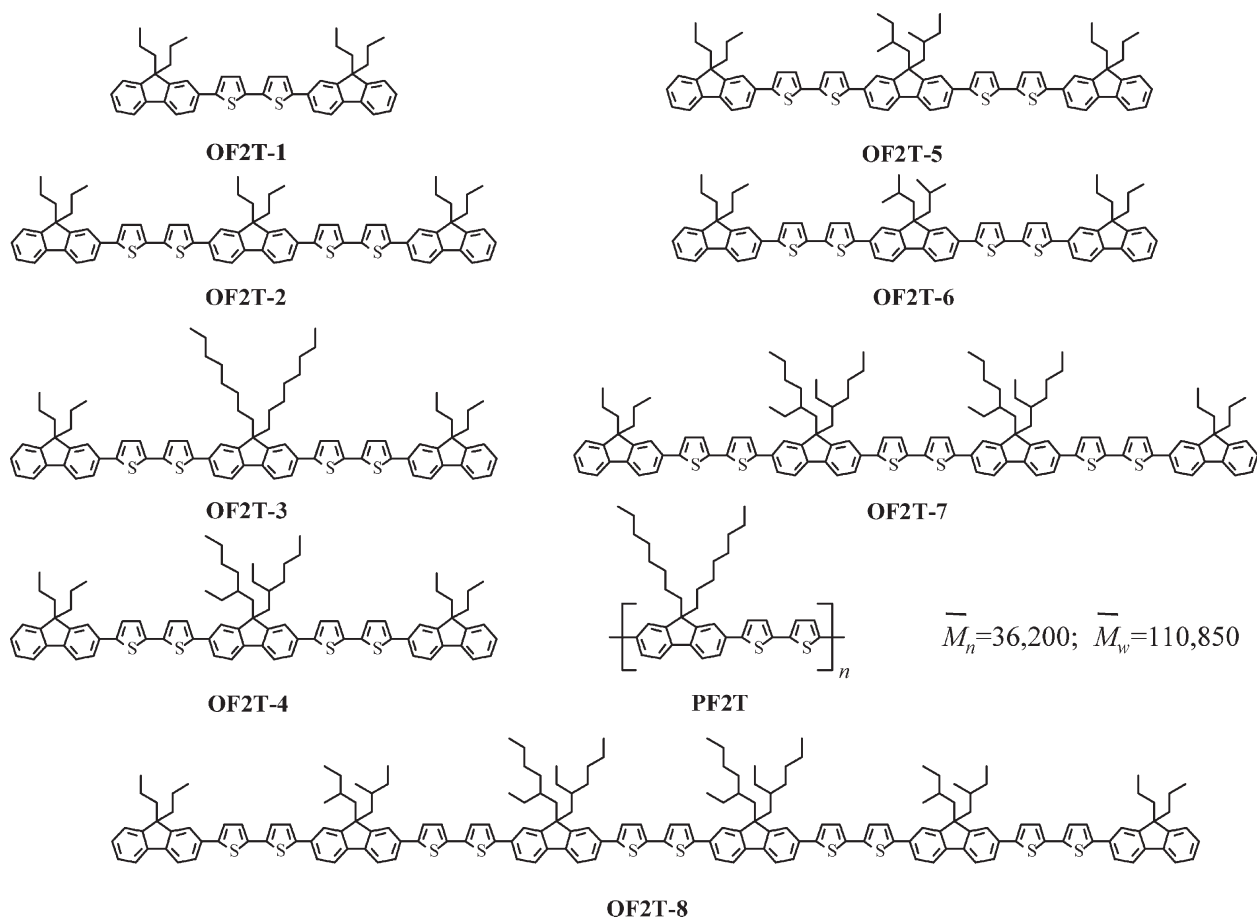
This study was motivated to unravel the roles played by the backbone length and aliphatic pendants to fluorene units' C-9 positions in thermotropic properties and morphological stability through the synthesis and characterization of a series OF2Ts. Top-gate field-effect transistors are constructed for the characterization of hole mobility using morphologically stable glassy-nematic materials. Particularly relevant to flexible electronics, solvent annealing at room temperature is being conducted in an attempt to emulate thermal annealing for producing monodomain glassy-nematic films.

2. Results and Discussion

Depicted in Scheme 1 are the molecular structures of oligo(fluorene-co-bithiophene)s, identified as OF2T-1 through -8,

synthesized for the present study. For a comparison with OF2Ts, commercially available PF2T is included in Scheme 1 accompanied by its number- and weight-average molecular weights, \bar{M}_n and \bar{M}_w . As compiled in Figure 1, the differential scanning calorimetric (DSC) thermograms of samples preheated to above whichever is higher—the crystalline melting point, T_m , or nematic-to-isotropic transition temperature, T_c —were used in conjunction with hot-stage polarizing optical microscopy for the determination of their thermotropic properties. A compound is classified as glassy-nematic if it exhibits a glass transition temperature, T_g , followed by a T_c on heating, and a T_c followed by a T_g on cooling without experiencing crystalline melting or crystallization.

Two structural parameters, the oligomer length and aliphatic pendants, affect the ability of an OF2T to form a morphologically stable glassy-nematic film. With four *n*-propyl pendants at the C-9 positions of the two fluorene units, OF2T-1 is an amorphous solid but prone to crystallization. Oligomers OF2T-2 through -6 incorporate an additional fluorene-bithiophene unit to OF2T-1. As revealed by the DSC thermograms, replacing linear aliphatic pendants to the C-9 position of the central fluorene unit with branched counterparts managed to improve morphological stability against crystallization, as glassy-nematic OF2T-4 and -5 are compared to OF2T-2 and -3. Note the lower T_g of OF2T-4 than that of OF2T-5, 97 versus 123 °C, with about the same T_c at



Scheme 1. Molecular structures of OF2T-1 through -8 and PF2T.

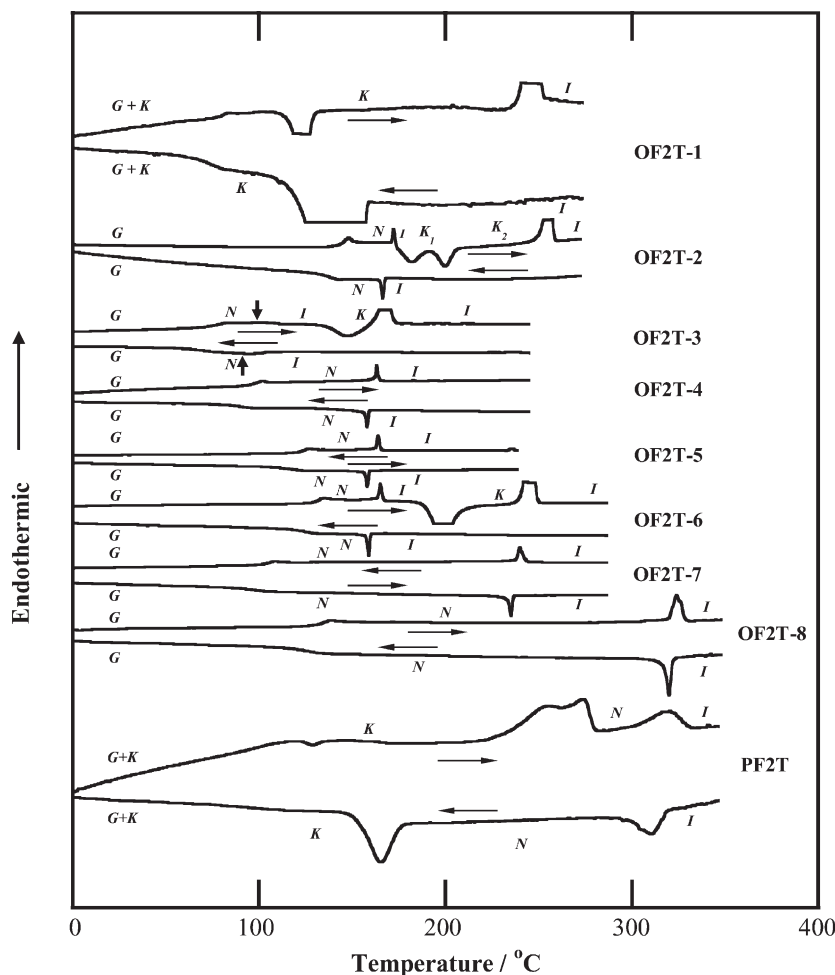


Figure 1. DSC thermograms at $\pm 20^\circ\text{C min}^{-1}$ for samples of OF2Ts and PF2T preheated to above T_c or T_m (whichever is higher) and then quenched to -30°C at $-100^\circ\text{C min}^{-1}$ before recording the reported second heating and cooling scans. Vertical arrows on the thermograms of OF2T-3 locate transition temperatures identified by hot-stage polarizing optical microscopy. Symbols: G, glassy; K, crystalline; N, nematic; I, isotropic.

164 °C thanks to the bulkier 2-ethylhexyl than the 2-methylbutyl pendants. Relatively compact 2-methylpropyl pendants, however, were ineffective in suppressing crystallization as evidenced by the DSC heating scan of OF2T-6, viz. thermally induced crystallization from isotropic liquid at 198 °C followed by crystalline melting at 245 °C. With an addition of one and two fluorene–bithiophene units to OF2T-5, OF2T-7, and -8 are both glassy-nematic systems with T_g at 102 and 133 °C and T_c at 240 and 324 °C, giving rise to a wide nematic fluid temperature range of 138 and 191 °C, respectively. The long-term morphological stability of glassy-nematic films of OF2T-7 and -8 were further ascertained by the absence of crystallization in spin-cast films left at room temperature for over a year. In sharp contrast to OF2T-7 and -8, PF2T exhibited complex thermal transition behaviors as shown in

Figure 1, including crystallization on heating and cooling under the same thermal treatment.

The UV–vis absorption and fluorescence spectra were gathered at 10^{-7} – 10^{-6} M in toluene. The results presented in Figure 2 show a red shift in both sets of spectra with increasing backbone length. Whereas the molar extinction coefficient, ϵ , increases by about $10^5 \text{ M}^{-1} \text{ cm}^{-1}$ with each increment of fluorene–bithiophene unit, a slight increase in fluorescence quantum yield, Φ_{PL} , with oligomer length is observed.^[44] The oxidation potentials were measured for OF2T-4, -5, -7, and -8 in anhydrous methylene chloride using the Ag/AgCl reference electrode and adjusted to ferrocene, which has an oxidation potential of 0.46 V relative to Ag/AgCl, for the calculation of HOMO levels using Equation 4 in Ref. [45], resulting in -5.3 ± 0.2 eV for all four oligomers. This procedure has been demonstrated to yield HOMO levels equivalent to direct measurement by ultraviolet photoemission spectroscopy.^[46] The data presented in Table 1 indicate the independence of HOMO level on the number of repeat units up to 52 in PF2T. Having a HOMO level at -5.3 ± 0.2 eV, OF2T-4 through -8 and PF2T represent an optimization between PF and poly(3-hexylthiophene) with respect to oxidative stability and ease of hole injection from gold.

Thin films of OF2Ts were spin-cast from chloroform onto fused-silica substrates containing rubbed polyimide alignment layers and then thermally annealed at 10 °C above their T_g s, viz. from 107 to 143 °C, for 5 min followed by cooling to room temperature. The resultant glassy-nematic films were monodomain across a 2-cm diameter, i.e., devoid of the Schlieren textures characteristic of nematic mesomorphism, as Figure 3b is compared to 3a. Linear absorption dichroism was characterized to evaluate the orientational order parameter, $S_{\text{ab}} = (R - 1)/$

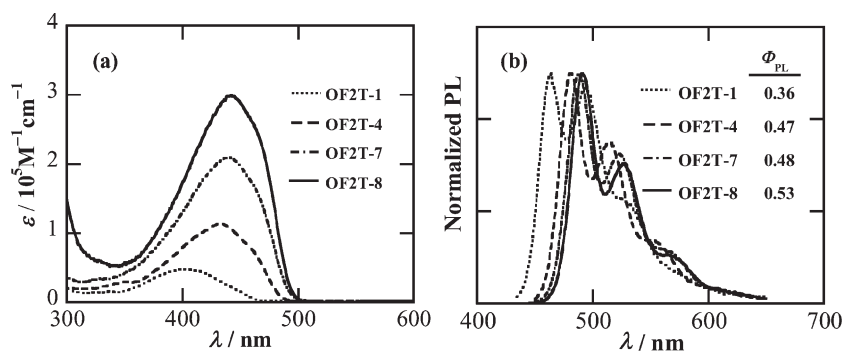


Figure 2. a) UV–Vis absorption spectra in molecular extinction coefficient, (ϵ ; and b) fluorescence (with excitation at 430 nm) spectra of OF2T-1, OF2T-4, OF2T-7, and OF2T-8 in toluene at 10^{-7} – 10^{-6} M.

Table 1. Highest occupied molecular orbital, HOMO, energy levels, orientational order parameters, S_{ab} , and anisotropic field-effect hole mobilities, $\mu_{||}$ and μ_{\perp} , for **OF2Ts** and **PF2T**.

Compound	HOMO [a] [eV]	S_{ab} [b]	$10^3 \mu_{ }$ [b] [$\text{cm}^2 \text{V}^{-1} \text{s}^{-1}$]	$10^3 \mu_{\perp}$ [b] [$\text{cm}^2 \text{V}^{-1} \text{s}^{-1}$]
OF2T-4	-5.4	0.78	0.56 ± 0.21	0.089 ± 0.034
OF2T-5	-5.4	0.76	0.43 ± 0.05	0.12 ± 0.02
OF2T-7	-5.3	0.82	1.8 ± 0.8	0.32 ± 0.14
OF2T-8	-5.3	0.84	2.0 ± 0.09	0.75 ± 0.43
PF2T	-5.3	0.70 [c]; 0.78 [d]	15 ± 5 [c]; 2 [d]	1.5 ± 0.5 [c]; 0.2 [d]

[a] The reported HOMO levels are accompanied by an uncertainty of ± 0.2 eV. [b] Orientational order parameter, S_{ab} , measured to ± 0.02 by polarized UV-Vis absorption, and anisotropic hole mobilities, $\mu_{||}$ and μ_{\perp} , measured for field-effect transistors, all comprising monodomain glassy-nematic films of **OF2Ts** spin-cast from chloroform on rubbed polyimide alignment coating and thermally annealed at 10°C above their respective T_g s for 5 min followed by cooling to room temperature. [c] Data taken from Ref. [21]. The **PF2T** film was thermally annealed at $275\text{--}285^\circ\text{C}$ for 3–15 min on rubbed polyimide film before cooling to room temperature, and poly(vinylphenol) served as the dielectric layer in a top-gate device. [d] Data taken from Ref. [25]. The **PF2T** film was thermally annealed at 280°C for 5 min on a photoalignment layer before cooling to room temperature, and the underlying SiO_2 served as the dielectric layer in a top-contact-bottom-gate device.

($R+2$), in which R denotes the absorbance parallel over that perpendicular to the nematic director defined by the rubbing direction. As reported in Table 1, the S_{ab} value increases from 0.76 to 0.84 with an increasing oligomer length. In contrast, the **PF2T** film exhibited an S_{ab} value of 0.70 and 0.60 after thermal annealing at $275\text{--}285^\circ\text{C}$ for 3–15 min on a rubbed polyimide layer^[21] and at 280°C for 5 min on a photoalignment layer,^[25] respectively. For the characterization of anisotropic hole mobilities, top-gate field-effect transistors as depicted in the Supporting Information were fabricated, in which monodomain glassy-nematic **OF2T** films were prepared by thermal annealing as described above with poly(chloro-*p*-xylylene) serving as the dielectric layer. Based on the source-drain current versus gate voltage relationships also included in the Supporting Information, hole mobilities were calculated in the saturation regime at a drain voltage of -100 V. As noted in Table 1, hole mobilities parallel ($\mu_{||}$) and perpendicular (μ_{\perp}) to the nematic director in the **OF2T** series generally increase with oligomer length but fall short of those of **PF2T** on a rubbed polyimide alignment layer,^[21] albeit comparable to **PF2T** on a photoalignment layer.^[25] Nonetheless, one should be cautious about comparing field-effect mobility data, as the results are known to be affected by device structure,^[6,7,47] alignment method,^[21,22,25] and the material used as the dielectric layer.^[8,9]

To take advantage of the relative ease of molecular alignment, monodisperse conjugated oligomers have been actively explored

as organic semiconductors capable of anisotropic charge transport. With singly defined molecular structures, monodisperse conjugated oligomers are invaluable to elucidating structure–property relationships. From a practical perspective, these compounds are readily soluble to facilitate purification and solution processing. In addition to thermal annealing, quasi-solvent annealing was tested in this study via spin coating from a high-boiling solvent on a rubbed polyimide alignment layer followed by vacuum drying, both performed at room temperature. The feasibility was demonstrated with **OF2T-8** spin-cast from chlorobenzene, resulting in $S_{ab} = 0.81$, a value very close to that from thermal annealing of a film spin-cast from chloroform, $S_{ab} = 0.84$; see Figure 4a and b. The success in quasi-solvent annealing of **OF2T-8** at room temperature originated in the oligomer's ability to undergo uniaxial orientation in a relatively wet environment thanks to the slow evaporation of chlorobenzene during spin coating. The attempt at quasi-solvent annealing of **OF2T-8** using low-boiling chloroform yielded an inferior S_{ab} at 0.33 as expected (see Fig. 4c). Presumably because of chain entanglements or defects as a result of its relatively high molecular weight, **PF2T** was irresponsive to quasi-solvent annealing using chlorobenzene as shown in Figure 4d.

Quasi-solvent annealing via spin coating of **OF2Ts** in chlorobenzene at 0.8 wt % and 3 000 rpm yielded a decreasing S_{ab} value with a decreasing solute length: 0.81, 0.77, and 0.52 for **OF2T-8**, -7, and -4, respectively, cf. Figures 4a, 5a, and b. Note the increasing departure of S_{ab} values at a decreasing oligomer length from those achieved with thermal annealing. Subsequent thermal annealing at 10°C above T_g s for 5 min improved the S_{ab} values to 0.85, 0.80, and 0.73 for **OF2T-8**, -7, and -4, respectively, equal to or slightly inferior to the results from thermal annealing. At the same mass concentration in chlorobenzene, the solution viscosity is expected to increase with an increasing oligomer length. Moreover, the depression in solvent-vapor pressure decreases with the molar concentration of an involatile solute, namely, a high solvent evaporation rate is expected of a long solute at the same mass concentration. The difference in evaporation rate, however, will diminish as spin coating proceeds. In this process, the difference in solution viscosity continues to grow beyond the initial value in favor of the long solute. Therefore, the longer the

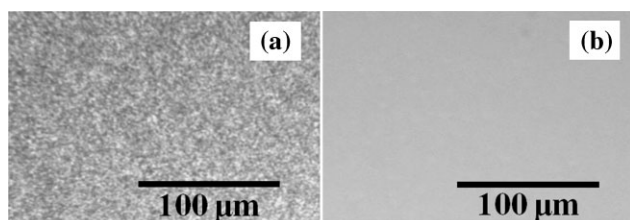


Figure 3. Polarizing optical micrographs of **OF2T-8** films spin-cast from chloroform on a rubbed polyimide alignment layer observed at 45° with respect to rubbing direction: a) pristine and b) after thermal annealing at 140°C for 5 min.

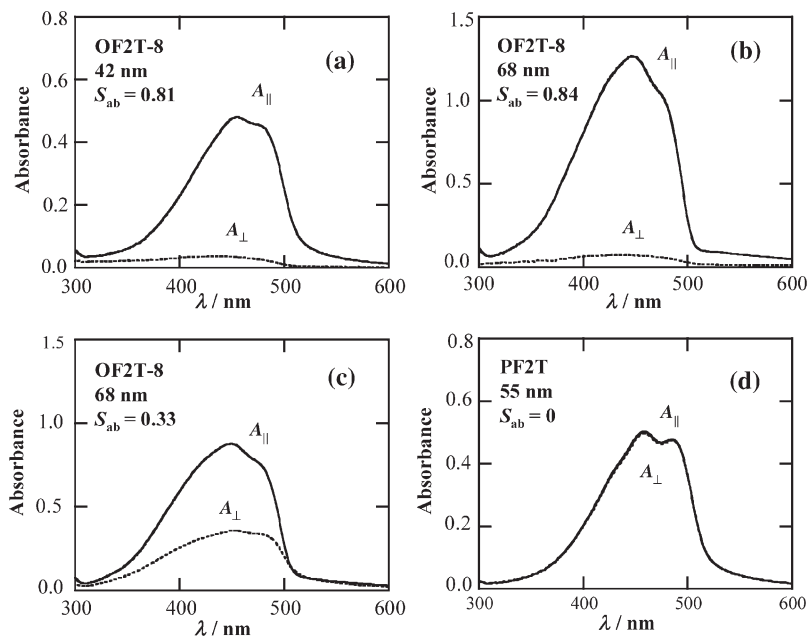


Figure 4. Polarized absorption spectra of films spin-cast from 0.8 wt % solutions at 3000 rpm for 65 s on rubbed polyimide alignment layers: a) **OF2T-8** film from chlorobenzene and then vacuum-dried at room temperature for up to 48 h; b) **OF2T-8** film from chloroform or chlorobenzene, thermally annealed at 140 °C for 5 min, and then cooled to room temperature; c) **OF2T-8** film from chloroform and then vacuum-dried at room temperature for 12 h; and d) **PF2T** film from chlorobenzene, and then vacuum-dried at room temperature for up to 48 h. The reported S_{ab} values are accompanied by an experimental error of ± 0.02 . Symbols $A_{||}$ and A_{\perp} represent absorbance parallel and perpendicular to rubbing direction, respectively.

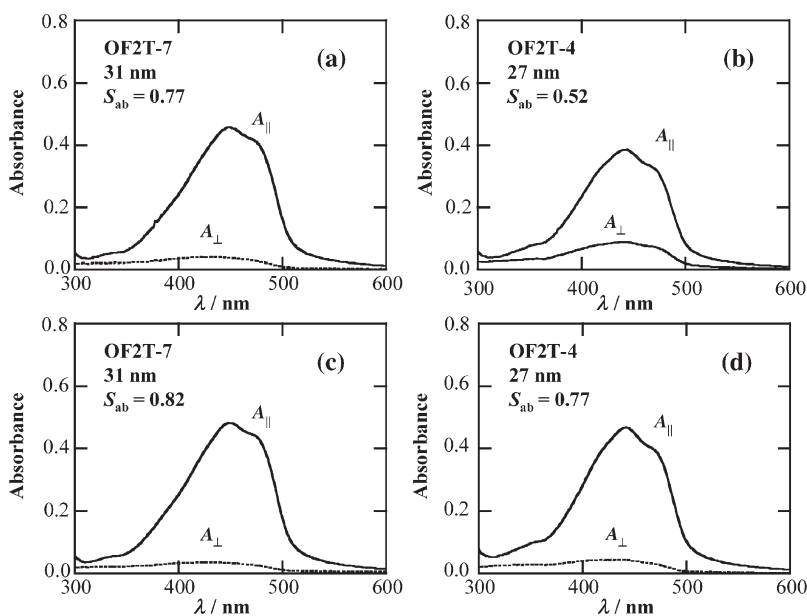


Figure 5. Polarized absorption spectra of films spin-cast from 0.8 wt % solutions at 3000 rpm for 65 s on rubbed polyimide alignment layers: a) **OF2T-7** film from chlorobenzene and then vacuum-dried at room temperature for up to 48 h; b) **OF2T-4** film from chlorobenzene and then vacuum-dried at room temperature for up to 48 h; c) **OF2T-7** film from chlorobenzene, followed by exposure to saturated chlorobenzene vapor for 30 s, and then vacuum-dried for up to 48 h, all at room temperature; d) **OF2T-4** film from chlorobenzene, followed by exposure to saturated chlorobenzene vapor for 30 s, and then vacuum-dried for up to 48 h, all at room temperature. The reported S_{ab} values are accompanied by an experimental error of ± 0.02 . Symbols $A_{||}$ and A_{\perp} are as defined in Figure 4.

solute, the thicker the liquid film with a higher solute mass concentration, and hence the thicker the dry oligomer film, as borne out by the experimental data: 55, 42, 31, and 27 nm for **PF2T**, **OF2T-8**, **-7**, and **-4**, respectively. The importance of solvent evaporation to dry film thickness is also evident by comparing chloroform with chlorobenzene as the solvents for spin coating. At the same **OF2T-8** mass concentration and spin rate as stated above, the thicker dry film from chloroform than chlorobenzene, 68 versus 42 nm, can be attributed to the higher solution viscosity during spin coating as a result of the higher evaporation rate of chloroform. In fact, the solvent evaporation rate seems to have predominated over the fact that chlorobenzene has a higher viscosity than chloroform, i.e., 0.80 over 0.54 cp at 20 °C.^[48]

In addition to quasi-solvent annealing, solvent-vapor annealing was conducted by exposing films spin-cast from chlorobenzene to saturated chlorobenzene vapor at room temperature for 30 s followed by vacuum drying also at room temperature up to 48 h. The resultant $S_{ab} = 0.82$ and 0.77 for **OF2T-7** and **-4**, as shown in Figure 5c and d, respectively, are identical with those attained with thermal annealing at 10 °C above their T_g s for 5 min (see Table 1). In comparison to solvent-vapor or thermal annealing, quasi-solvent annealing amounted to kinetically trapping the orientational order of **OF2Ts** in view of the generally lower S_{ab} values. The solvent-vapor annealing process can be described as permeation of an organic vapor into a spin-cast **OF2T** film to plasticize liquid crystal molecules for spontaneous self-organization motivated by the rubbed polyimide layer. As encountered in quasi-solvent annealing, a spin-cast **PF2T** film failed to be oriented by solvent-vapor annealing using chlorobenzene or chloroform from 30 s to 8 h. It should also be noted that both quasi-solvent annealing and solvent-vapor annealing using chlorobenzene followed by drying in vacuo, all at room temperature, produced monodomain glassy-nematic films of **OF2Ts** across a 2-cm diameter observed under polarizing optical microscopy with the same micrographs as that from thermal annealing shown in Figure 3b. Solvent annealing has been documented for performance enhancement of organic solar cells through modulation of nanoscale biphasic crystalline-amorphous morphology.^[49–54] Furthermore, solvent-vapor annealing has been shown to induce crystalline modification up to the millimeter scale for the improvement of field-effect mobility of a solution-processa-

ble organic semiconductor.^[55] The work reported here is the first demonstration of solvent annealing for the realization of monodomain glassy-nematic films of conjugated oligomers. Work is in progress to incorporate photoalignment on plastic substrates at room temperature prior to solvent annealing of conjugated oligomer films without resorting to high temperature baking of polyimide alignment layers.

3. Conclusions

A series of OF2Ts were synthesized and characterized to evaluate the effects of oligomer length and pendant aliphatic structures on thermotropic properties. The UV-vis absorption and fluorescence spectra were gathered in toluene, and the HOMO energy levels were calculated using the oxidation potentials measured by cyclic voltammetry in methylene chloride. Top-gate field-effect transistors comprising uniaxially aligned OF2T films were constructed for the characterization of anisotropic hole mobilities. In addition to the widely practiced thermal annealing to attain monodomain glassy-nematic films, two approaches to solvent annealing were explored at room temperature. Key observations are recapitulated as follows:

- 1) For a given oligomer length, branched aliphatic pendants are more effective than linear pendants in suppressing crystallization. For the relatively short oligomer consisting of two repeat units end-capped with fluorene, the 2-methylbutyl group has emerged as the optimum branched pendant compared to 2-ethylhexyl and 2-methylpropyl groups in terms of glass-transition temperature and resistance to crystallization. With a T_g at 102 and 133 °C and a T_c at 240 and 324 °C, respectively, oligomers comprising three and five repeat units also end-capped with fluorene are capable of forming glassy-nematic films without encountering crystallization at room temperature for over a year.
- 2) At an increasing oligomer length, the light absorption and fluorescence spectra in toluene undergo a bathochromic shift accompanied by a substantial enhancement in molar extinction coefficient but a modest increase in fluorescence quantum yield. The HOMO energy levels are constant at -5.3 ± 0.2 eV for all OF2Ts and PF2T with 52 number-average repeat units. Field-effect hole mobilities increase with oligomer length but fall short of those of PF2T on a rubbed polyimide alignment layer, albeit comparable to PF2T on a photoalignment layer.
- 3) Quasi-solvent annealing of OF2Ts and PF2T films via spin coating from chlorobenzene at the same mass concentration and spin rate produced kinetically trapped S_{ab} values in dry films with thicknesses that decrease with a decreasing oligomer length. Solvent-vapor annealing was performed by exposing spin-cast films to saturated chlorobenzene vapor at room temperature, yielding S_{ab} values identical to those from thermal annealing. Both approaches to solvent annealing produced monodomain glassy-nematic films across a 2-cm diameter, as did thermal annealing. While amenable to thermal annealing at an elevated temperature, PF2T was not responsive at all to either approach of solvent annealing.

4. Experimental

Materials Synthesis and Purification Procedures: All chemicals, reagents, and solvents were used as received from commercial sources without further purification except tetrahydrofuran (THF) and toluene, which were distilled over sodium/benzophenone before use. The target compounds were synthesized and purified according to Scheme 2 following the procedures described below. All reactions were carried out under argon atmosphere and anhydrous conditions unless noted otherwise. Intermediates **1**, **5a–e**, and **12** were synthesized according to the procedures reported previously [31–33]. PF2T was acquired from American Dye Source (Quebec, Canada) with a number-average molecular weight of 36200 g mol⁻¹ and a polydispersity index of 3.1.

5-[9,9-Bis(*n*-propyl)fluoren-2-yl]-2,2'-bithiophene, 3: A Grignard reagent, **2**, prepared by reacting 5-bromo-2,2'-bithiophene (4 g, 16.3 mmol) with Mg (0.6 g, 25 mmol) in THF (80 mL), was added dropwise into a solution of 2-bromo-[9,9-bis(*n*-propyl)]-fluorene (**1**, 4.12 g, 12.5 mmol) in THF (30 mL) containing Pd(dppf)Cl₂ (90 mg, 1.3 mmol) as a catalyst. The reaction mixture was stirred at room temperature overnight, quenched with 0.2 M HCl, and extracted with methylene chloride. The organic extracts were combined, washed with brine and water, and finally dried over MgSO₄. Upon evaporating off the solvent, the crude product was purified by column chromatography on silica gel with hexane as the eluent to yield **3** (0.75 g, 86%) as yellow crystals. ¹H NMR (400 MHz, CDCl₃, 298 K): δ (ppm) 7.70–7.68 (d, $J = 4.4$ Hz, 2H), 7.59–7.55 (m, 2H), 7.36–7.29 (m, 4H), 7.23–7.22 (m, 2H), 7.18–7.17 (d, $J = 3.6$ Hz, 1H), 7.06–7.03 (m, 1H), 2.00–1.96 (m, 4H), 0.73–0.67 (m, 10H).

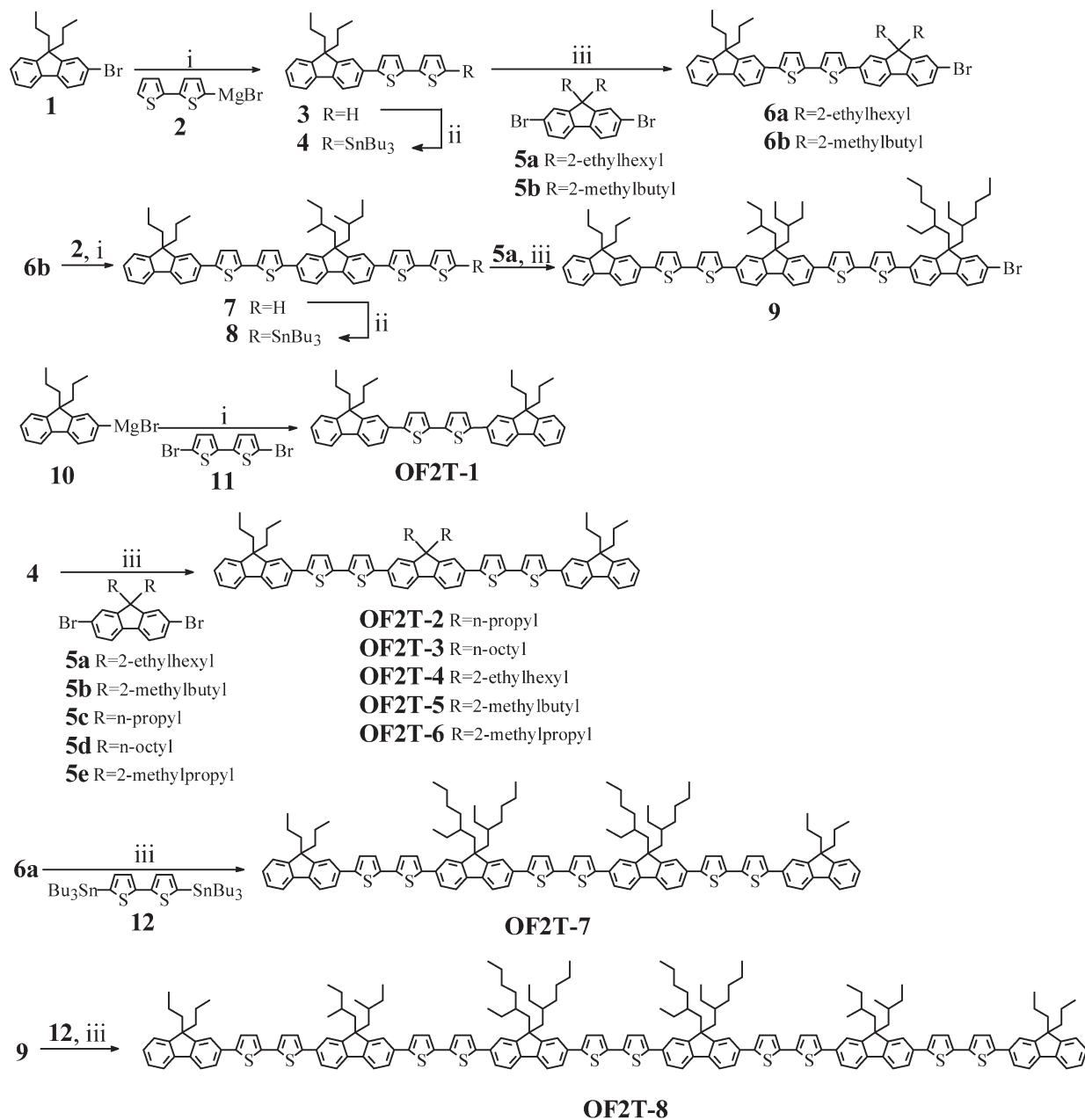
5-[9,9-Bis(*n*-propyl)fluoren-2-yl]-5'-tributylstanyl-2,2'-bithiophene, 4: Into a stirred solution of **3** (1.24 g, 3 mmol) in THF (30 mL) was added *n*-BuLi (2.5 M in hexane, 1.6 mL, 4.0 mmol) dropwise at -78 °C, where the reaction mixture was stirred for 3 h before adding tributylstannyl chloride (1.3 g, 4 mmol) in one portion. The reaction mixture was allowed to warm up to room temperature overnight before pouring into water for extraction with diethylether. The organic extracts were combined, washed with brine and water, and dried over MgSO₄. Upon evaporating off the solvent, **4** was obtained in a quantitative yield. ¹H NMR (400 MHz, CDCl₃, 298 K): δ (ppm) 7.69–7.67 (m, 2H), 7.59–7.55 (m, 2H), 7.34–7.28 (m, 6H), 7.18–7.16 (d, $J = 4.0$ Hz, 1H), 7.10–7.08 (d, $J = 3.2$ Hz, 1H), 1.98–1.95 (m, 4H), 1.65–0.93 (m, 27H), 0.77–0.69 (m, 10H).

5-[9,9-Bis(*n*-propyl)fluoren-2-yl]-5'-[7-bromo-9,9-bis(2-ethylhexyl)fluoren-2-yl]-2,2'-bithiophene, 6a: Toluene (50 mL) was added to a mixture of **4** (3.52 g, 5 mmol), 2,7-dibromo-9,9-bis(2-ethylhexyl)-fluorene (**5a**) (6.85 g, 12.5 mmol), and Pd(PPh₃)₄ (60 mg, 0.05 mmol). The reaction mixture was stirred at 90 °C overnight. Upon evaporating off the solvent, the crude product was purified by gradient column chromatography on silica gel with hexane:methylene chloride at 20:1 to 9:1 (v/v) as the eluent to yield **6a** (2.3 g, 52%) as a yellow solid. ¹H NMR (400 MHz, CDCl₃, 298 K): δ (ppm) 7.71–7.46 (m, 10H), 7.35–7.30 (m, 5H), 7.23–7.22 (d, $J = 3.6$ Hz, 2H), 2.13–2.00 (m, 8H), 0.98–0.72 (m, 32H), 0.63–0.58 (m, 8H).

5-[9,9-Bis(*n*-propyl)fluoren-2-yl]-5'-[7-bromo-9,9-bis(2-methylbutyl)fluoren-2-yl]-2,2'-bithiophene, 6b: The procedure for the synthesis of **6a** was followed to prepare **6b** from **4** and 2,7-dibromo-9,9-bis(2-methylbutyl)-fluorene (**5b**) as a yellow solid in a 57% yield. ¹H NMR (400 MHz, CDCl₃, 298 K): δ (ppm) 7.71–7.46 (m, 10H), 7.35–7.30 (m, 5H), 7.23–7.22 (d, $J = 3.6$ Hz, 2H), 2.25–1.86 (m, 8H), 1.05–0.62 (m, 22H), 0.45–0.30 (m, 6H).

2-[5'-[9,9-Bis(*n*-propyl)fluoren-2-yl]-2,2'-bithiophen-5-yl]-7-(2,2'-bithiophen-5-yl)-9,9-bis(2-methylbutyl)fluorene, 7: The procedure for the synthesis of **3** was followed to prepare **7** from **6b** and **2** as a yellow solid in a 75% yield. ¹H NMR (400 MHz, CDCl₃, 298 K): δ (ppm) 7.71–7.57 (m, 10H), 7.37–7.27 (m, 6H), 7.24–7.22 (m, 4H), 7.19–7.18 (d, $J = 4.0$ Hz, 1H), 7.06–7.03 (m, 1H), 2.20–1.86 (m, 8H), 1.05–0.62 (m, 22H), 0.40–0.30 (m, 6H).

2-[5'-[9,9-Bis(*n*-propyl)fluoren-2-yl]-2,2'-bithiophen-5-yl]-7-(5'-tributylstanyl-2,2'-bithiophen-5-yl)-9,9-bis(2-methylbutyl)fluorene, 8: The procedure for the synthesis of **4** was followed to prepare **8** from **7** in a quantitative yield. ¹H NMR (400 MHz, CDCl₃, 298 K): δ (ppm) 7.71–7.57 (m, 10H), 7.37–7.27 (m, 7H), 7.23–7.22 (m, 2H), 7.18–7.17 (d, $J = 3.6$ Hz, 1H), 7.10–7.09 (d,



(i) Pd(dppf)Cl₂, THF, room temperature. (ii) BuLi, THF, -78°C and then SnBu₃Cl, -78°C to room temperature; (iii) Pd(PPh₃)₄, toluene, 90°C.

Scheme 2. Synthesis of OF2T-1 through -8 as depicted in Scheme 1.

$J = 3.2$ Hz, 1H), 2.25–1.86 (m, 8H), 1.65–0.60 (m, 49H), 0.45–0.30 (m, 6H).

2-[5'-[9,9-Bis(*n*-propyl)fluoren-2-yl]-2,2'-bithiophen-5-yl]-7-(5'-[7-bromo-9,9-bis(2-ethyl-hexyl)fluoren-2-yl]-2,2'-bithiophen-5-yl)-9,9-bis(2-methylbutyl)fluorene, **9**: The procedure for the synthesis of **6a** was followed to prepare **9** from **8** and **5a** as a yellow solid in a 51% yield. ¹H NMR (400 MHz, CDCl₃, 298 K): δ (ppm) 7.74–7.44 (m, 16H), 7.40–7.30 (m, 7H), 7.23–7.21 (m, 4H), 2.25–1.86 (m, 12H), 1.05–0.62 (m, 54H), 0.45–0.30 (m, 6H).

5,5'-Bis[9,9-bis(*n*-propyl)fluoren-2-yl]-2,2'-bithiophene, **OF2T-1**: A Grignard reagent, **10**, prepared by the reaction of 2-bromo-[9,9-bis(*n*-propyl)-

fluorene (0.99 g, 3 mmol) with Mg (0.08 g, 3.3 mmol) in THF (10 mL), was added dropwise into a stirred solution of 5,5'-dibromo-2,2'-bithiophene (**11**, 0.40 g, 1.2 mmol) in THF (20 mL) containing Pd(dppf)Cl₂ (20 mg, 0.03 mmol) as a catalyst. The reaction mixture was stirred at room temperature overnight, quenched with 0.2 M HCl, and extracted with methylene chloride. The organic extracts were combined, washed with brine and water, and dried over MgSO₄. Upon evaporating off the solvent, the crude product was purified by gradient column chromatography on silica gel with hexane:methylene chloride at 10:0 to 9:1 (v/v) as the eluent to yield **OF2T-1** (0.75 g, 86%) as a yellow powder. ¹H NMR (400 MHz, CDCl₃, 298 K): δ (ppm) 7.71–7.69 (m, 4H), 7.61–7.57 (m, 4H), 7.37–7.30 (m, 8H),

7.23–7.22 (d, $J = 3.6$ Hz, 2H), 2.01–1.98 (m, 8H), 0.73–0.69 (m, 20H). MALD/I TOF MS (DCTB) m/z ($[M]^+$): 662.3. Calcd for $C_{46}H_{46}S_2$: C, 83.34; H, 6.99. Found: C, 83.12; H, 6.92.

2,7-Bis[5'-[9,9-bis(n-propyl)fluoren-2-yl]-2,2'-bithiophen-5-yl]-9,9-bis(n-propyl)fluorene, OF2T-2: Toluene (20 mL) was added into a mixture of **4** (2.47 g, 3.5 mmol), 2,7-dibromo-9,9-bis(n-propyl)-fluorene (**5c**) (0.49 g, 1.2 mmol) and $Pd(PPh_3)_4$ (90 mg, 0.075 mmol). The reaction mixture was stirred at 90 °C overnight. Upon evaporating off the solvent, the crude product was purified by gradient column chromatography on silica gel with hexane:methylene chloride at 4:1 to 2:1 (v/v) as the eluent to give **OF2T-2** (0.76 g, 58%) as a yellow powder. 1H NMR (400 MHz, $CDCl_3$, 298 K): δ (ppm) 7.71–7.69 (m, 6H), 7.63–7.57 (m, 8H), 7.36–7.31 (m, 10H), 7.24–7.23 (d, $J = 3.6$ Hz, 4H), 2.04–1.98 (m, 12H), 0.73–0.69 (m, 30H). MALD/I TOF MS (DCTB) m/z ($[M]^+$): 1074.5. Calcd for $C_{73}H_{70}S_4$: C, 81.52; H, 6.56. Found: C, 81.24; H, 6.41.

2,7-Bis[5'-[9,9-bis(n-propyl)fluoren-2-yl]-2,2'-bithiophen-5-yl]-9,9-bis(n-octyl)fluorene, OF2T-3: The procedure for the synthesis of **OF2T-2** was followed to prepare **OF2T-3** from **4** and 2,7-dibromo-9,9-bis(n-octyl)fluorene (**5d**) as a yellow powder in a 69% yield. 1H NMR (400 MHz, $CDCl_3$, 298 K): δ (ppm) 7.71–7.69 (m, 6H), 7.63–7.57 (m, 8H), 7.36–7.31 (m, 10H), 7.24–7.23 (d, $J = 3.6$ Hz, 4H), 2.02–1.98 (m, 12H), 1.18–1.09 (m, 20H), 0.85–0.78 (m, 30H). MALD/I TOF MS (dithranol) m/z ($[M]^+$): 1214.4. Calcd for $C_{83}H_{90}S_4$: C, 81.99; H, 7.46. Found: C, 81.65; H, 7.26.

2,7-Bis[5'-[9,9-bis(n-propyl)fluoren-2-yl]-2,2'-bithiophen-5-yl]-9,9-bis(2-ethyl-hexyl)fluorene, OF2T-4: The procedure for the synthesis of **OF2T-2** was followed to prepare **OF2T-4** from **4** and **5a** as a yellow powder in a 72% yield. 1H NMR (400 MHz, $CDCl_3$, 298 K): δ (ppm) 7.71–7.69 (m, 6H), 7.62–7.58 (m, 8H), 7.36–7.29 (m, 10H), 7.23–7.22 (d, $J = 4.0$ Hz, 4H), 2.08–1.98 (m, 12H), 0.93–0.55 (m, 50H). MALD/I TOF MS (DCTB) m/z ($[M]^+$): 1214.7. Calcd for $C_{83}H_{90}S_4$: C, 81.99; H, 7.46. Found: C, 82.08; H, 7.28.

2,7-Bis[5'-[9,9-bis(n-propyl)fluoren-2-yl]-2,2'-bithiophen-5-yl]-9,9-bis(2-methyl-butyl)fluorene, OF2T-5: The procedure for the synthesis of **OF2T-2** was followed to prepare **OF2T-5** from **4** and **5b** as a yellow powder in a 59% yield. 1H NMR (400 MHz, $CDCl_3$, 298 K): δ (ppm) 7.72–7.69 (m, 6H), 7.63–7.57 (m, 8H), 7.36–7.31 (m, 10H), 7.24–7.23 (d, $J = 3.6$ Hz, 4H), 2.21–2.18 (m, 2H), 2.02–1.98 (m, 10H), 0.93–0.80 (m, 4H), 0.78–0.61 (m, 28H), 0.35–0.30 (m, 6H). MALD/I TOF MS (DCTB) m/z ($[M]^+$): 1130.4. Calcd for $C_{77}H_{78}S_4$: C, 81.72; H, 6.95. Found: C, 81.30; H, 6.78.

2,7-Bis[5'-[9,9-bis(n-propyl)fluoren-2-yl]-2,2'-bithiophen-5-yl]-9,9-bis(2-methyl-propyl)fluorene, OF2T-6: The procedure for the synthesis of **OF2T-2** was followed to prepare **OF2T-6** from **4** and 2,7-dibromo-9,9-bis(2-methylpropyl)-fluorene (**5e**) as a yellow powder in a 80% yield. 1H NMR (400 MHz, $CDCl_3$, 298 K): δ (ppm) 7.73–7.69 (m, 6H), 7.64–7.57 (m, 8H), 7.36–7.31 (m, 10H), 7.24–7.23 (d, $J = 4.0$ Hz, 4H), 2.07–1.98 (m, 12H), 1.03–0.95 (m, 2H), 0.73–0.69 (m, 20H), 0.46–0.45 (d, $J = 6.8$ Hz, 12H). MALD/I TOF MS (DCTB) m/z ($[M]^+$): 1102.4. Calcd for $C_{75}H_{74}S_4$: C 81.62 H 6.76. Found: C, 81.49; H, 6.56.

5,5'-Bis[7-[5'-[9,9-bis(n-propyl)fluoren-2-yl]-2,2'-bithiophen-2-yl]-9',9'-bis(2-ethyl-hexyl)fluoren-2-yl]-2,2'-bithiophene, OF2T-7: Toluene (20 mL) was added into a mixture of **6a** (1.94 g, 2.2 mmol), 5,5'-tributylstanyl-2,2'-bithiophene (**12**) (0.56 g, 0.8 mmol), and $Pd(PPh_3)_4$ (90 mg, 0.060 mmol). The reaction mixture was stirred at 90 °C overnight. Upon evaporating off the solvent, the crude product was purified by gradient column chromatography on silica gel with hexane:methylene chloride at 4:1 to 2:1 (v/v) as the eluent to yield **OF2T-7** (0.95 g, 67%) as a yellow powder. 1H NMR (400 MHz, $CDCl_3$, 298 K): δ (ppm) 7.71–7.69 (m, 8H), 7.62–7.58 (m, 12H), 7.37–7.30 (m, 12H), 7.23–7.22 (d, $J = 3.6$ Hz, 6H), 2.08–2.00 (m, 16H), 0.94–0.53 (m, 80H). MALD/I TOF MS (DCTB) m/z ($[M]^+$): 1767.9. Calcd for $C_{120}H_{134}S_6$: C, 81.49; H 7.64. Found: C, 81.21; H, 7.64.

5,5-Bis[7-(5'-[7-(5'-[9,9-bis(n-propyl)fluoren-2-yl]-2,2'-bithiophen-5-yl)-9,9-bis(2-methyl-butyl)fluoren-2-yl]-2,2'-bithiophen-5-yl)-9,9-bis(2-ethylhexyl)fluoren-2-yl]-2,2'-bithiophene, OF2T-8: The procedure for the synthesis of **OF2T-7** was followed to synthesize **OF2T-8** from **9** and **12** as a yellow powder in a 63% yield. 1H NMR (400 MHz, $CDCl_3$, 298K): δ (ppm) 7.72–7.58 (m, 32H), 7.38–7.29 (m, 16H), 7.24–7.23 (m, 10H), 2.30–1.96 (m, 24H), 1.05–0.57 (m, 104H), 0.45–0.35 (m, 12H). MALD/I TOF MS (DCTB) m/z ($[M]^+$): 2703.3. Calcd for $C_{182}H_{198}S_{10}$: C, 80.78; H 7.37. Found: C, 80.46; H, 7.27.

Molecular Structures, Morphology, and Phase Transition Temperatures: 1H NMR spectra were acquired in $CDCl_3$ with an Avance-400 spectrometer (400 MHz). Elemental analysis was carried out by Quantitative Technology, Inc. Molecular weights were measured with a ToFSpec2E MALD/I TOF mass spectrometer (Micromass, Inc., Manchester, UK) with 2-[(2E)-3-(4-tert-butylphenyl)-2-methylpropenyldiene]malonitrile (DCTB) as the matrix. Thermal transition temperatures were determined by differential scanning calorimetry (Perkin-Elmer DSC-7) with a continuous N_2 purge at $20 mL min^{-1}$. Samples were preheated to above T_c or T_m (whichever is higher) and then cooled down $-30^\circ C$ at $-100^\circ C min^{-1}$ before the reported second heating and cooling scans were recorded at $\pm 20^\circ C min^{-1}$. The nature of phase transition was characterized by hot-stage polarizing optical microscopy (DMLM, Leica, FP90 central processor and FP82 hotstage, Mettler Toledo).

Absorption and Fluorescence Spectra in Dilute Solution: Dilute solutions of **OF2Ts** in toluene were prepared at a concentration of 10^{-7} – 10^{-6} M. Absorption spectra were acquired with an HP 8453E UV–Vis–NIR diode array spectrophotometer. Fluorescence spectra were collected with a spectrofluorimeter (Quanta Master C60SE, Photon Technology International) at an excitation wavelength of 430 nm. The fluorescence quantum yield of **OF2Ts** in diluted solution was measured following the procedure reported previously [33].

Electrochemical Characterization: Cyclic voltammetry was conducted on an EC-Epsilon potentiostat (Bioanalytical Systems, Inc.) at a concentration of 10^{-4} M in anhydrous dichloromethane containing 0.1 M tetraethylammonium tetrafluoroborate as the supporting electrolyte. A silver/silver chloride wire (2 mm diameter), a platinum wire (0.5 mm diameter), and a platinum disk (1.6 mm diameter) were used as the reference, counter, and working electrodes, respectively, to complete a standard 3-electrode cell. Prior to use, the supporting electrolyte was dissolved in a minimum amount of ethanol for treatment with activated charcoal followed by filtration through Celite powder and addition of water (twice the volume of the ethanol) for recrystallization at 0 °C. Recrystallization was repeated until the oxidation and reduction scans attributable solely to the electrolyte were observed. The difference between the oxidation potential of **OF2Ts** and that of ferrocene, both against Ag/AgCl, were used as the oxidation potential of **OF2Ts** over Fc/Fc^+ ($Fc = ferrocene$) [56]. HOMO levels of the **OF2Ts** were calculated via $HOMO = -(1.4 \pm 0.1) \times qV_{CV} - (4.6 \pm 0.08) eV$, where q is the electron charge, V_{CV} is the oxidation potential of an **OF2T** over Fc/Fc^+ [45].

Preparation and Characterization of Neat Films: Optically flat fused-silica substrates (25.4 mm diameter \times 3 mm thickness, transparent down to 200 nm, Esco Products) were coated with a thin film of polyimide (Nissan SUNEVER grade 610 polyimide varnish) following by soft-baking at 80 °C for 10 min and hard-curing at 250 °C for 1 h, and uniaxial rubbing for use as an alignment layer. Films of **OF2Ts** were prepared by spin coating from a dilute solution onto fused-silica substrates containing alignment coatings at 3000 rpm for 65 s followed by drying under vacuum overnight. The solution concentration was adjusted to control the film thickness to within 50–70 nm. Thermal annealing was performed under argon atmosphere at a temperature 10 °C above the glass transition temperature for 5 min. Quasi-solvent annealing was performed by spin coating from a 0.8 wt % solution in chlorobenzene at 3000 rpm for 65 s followed by drying under vacuum for up to 48 h. Solvent-vapor annealing was executed by exposing spin-cast films from chlorobenzene to saturated chlorobenzene vapor in a closed jar for a varying period of time before drying under vacuum for up to 48 h, all conducted at room temperature. Absorption dichroism was characterized by a UV–Vis–NIR spectrophotometer (Perkin-Elmer Lambda 900) equipped with linear polarizers (HNP'B, Polaroid) for the calculation of orientational order parameter. Film thickness was measured by optical profilometry (Zygo NewView 5000).

Fabrication and Characterization of Field-Effect Transistors: The 40-nm-thick gold source/drain electrodes were deposited by evaporation through a shadow mask onto a rubbed polyimide layer as a part of the top-gate field-effect transistor with channel lengths ranging from 75 to 120 μm . The **OF2T** films were spin cast from chloroform, vacuum dried, and thermally annealed as described above. A 500–800 nm thick, poly(chloro-*p*-xylylene) film was prepared on top of the **OF2T** film by chemical vapor deposition to

serve as the gate insulator [57]. Device fabrication was completed by evaporation of a 30–40-nm-thick gold gate electrode through a shadow mask, resulting in a channel width of 5 nm. The finished device structure is sketched in Figure S-18. The thickness of the evaporated gate insulator was measured with a profilometer (Sloan Dektak 3). The current–voltage characteristics of the resultant transistors were characterized with an Agilent 4156C precision semiconductor parameter analyzer in ambient atmosphere. Hole mobilities were calculated in the saturation regime at a drain voltage of -100 V using the standard MOSFET equations [47].

Acknowledgements

The authors thank Kevin Klubek and Andrew J. Hotelling of Eastman Kodak Company for MALD/I-TOF analysis, Diane Freeman and David Levy (Eastman Kodak Company) for assistance in OFET device fabrication and measurement, and Kenneth L. Marshall of the Laboratory for Laser Energetics, LLE, at University of Rochester for helpful discussions and technical advice. They are grateful for the financial support provided by the New York State Energy Research and Development Authority. Additional funding was provided by the Department of Energy Office of Inertial Confinement Fusion under Cooperative Agreement No. DE-FC52-08NA28302 with LLE. Supporting Information is available online from Wiley InterScience or from the authors.

Received: January 20, 2009
Published online: May 5, 2009

- [1] K. Müllen, G. Wegner, *Electronic Materials: The Oligomer Approach*, Wiley-VCH, Weinheim, Germany **1998**.
- [2] G. Hadziioannou, P. F. van Hutten, *Semiconducting Polymers Chemistry, Physics and Engineering*, Wiley-VCH, Weinheim, Germany **2000**.
- [3] K. Müllen, U. Scherf, *Organic Light Emitting Devices: Synthesis, Properties and Applications*, Wiley-VCH, Weinheim, Germany **2006**.
- [4] H. Klauk, *Organic Electronics: Materials, Manufacturing and Applications*, Wiley-VCH, Weinheim, Germany **2006**.
- [5] Y. Shirota, H. Kagenyma, *Chem. Rev.* **2007**, *107*, 953.
- [6] T. W. Kelley, P. F. Baude, C. Gerlach, D. E. Ender, D. Muires, M. A. Haase, D. E. Vogel, S. D. Theiss, *Chem. Mater.* **2004**, *16*, 4413.
- [7] C. R. Newman, C. D. Frisbie, D. A. da Silva Filho, J.-L. Brédas, P. C. Ewbank, K. R. Mann, *Chem. Mater.* **2004**, *16*, 4436.
- [8] J. Veres, S. Ogier, G. Lloyd, D. de Leeuw, *Chem. Mater.* **2004**, *16*, 4543.
- [9] A. Facchetti, M.-H. Yoon, T. J. Marks, *Adv. Mater.* **2005**, *17*, 1705.
- [10] A. R. Murphy, J. M. J. Fréchet, *Chem. Rev.* **2007**, *107*, 1066.
- [11] S. Allard, M. Forster, B. Souharce, H. Thiem, U. Scherf, *Angew. Chem. Int. Ed.* **2008**, *47*, 4070.
- [12] M. Grell, D. D. C. Bradley, *Adv. Mater.* **1999**, *11*, 895.
- [13] T. Miteva, A. Miesel, W. Knoll, H. G. Nothofer, U. Scherf, D. C. Müller, K. Meerholz, A. Yasuda, D. Neher, *Adv. Mater.* **2001**, *13*, 565.
- [14] D. Neher, *Macromol. Rapid Commun.* **2001**, *22*, 1365.
- [15] D. Sainova, A. Zen, H.-G. Nothofer, U. Asawapirom, U. Scherf, R. Hagen, T. Biringier, S. Kostromine, D. Neher, *Adv. Funct. Mater.* **2002**, *12*, 49.
- [16] M. Misaki, Y. Ueda, S. Nagamatsu, M. Chikamatsu, Y. Yoshida, N. Tanigaki, K. Yase, *Appl. Phys. Lett.* **2005**, *87*, 243503.
- [17] M. Knaapila, R. Stepanyan, B. P. Lyons, M. Torkkeli, A. P. Monkman, *Adv. Funct. Mater.* **2006**, *19*, 599.
- [18] K. Sakamoto, K. Miki, M. Misaki, K. Sakaguchi, M. Chikamatsu, R. Azumi, *Appl. Phys. Lett.* **2007**, *91*, 183509.
- [19] M. Misaki, M. Chikamatsu, Y. Yoshida, R. Azumi, N. Tanigaki, K. Yase, S. Nagamatsu, Y. Ueda, *Appl. Phys. Lett.* **2008**, *93*, 023304.
- [20] D. O'Carroll, G. Redmond, *Chem. Mater.* **2008**, *20*, 6501.
- [21] H. Sirringhaus, R. J. Wilson, R. H. Friend, M. Inbasekaran, W. Wu, E. P. Woo, M. Grell, D. D. C. Bradley, *Appl. Phys. Lett.* **2000**, *77*, 406.
- [22] S. P. Li, C. J. Newsome, D. M. Russell, T. Kugler, M. Ishida, T. Shimoda, *Appl. Phys. Lett.* **2005**, *87*, 062101.
- [23] L. R. Pattison, A. Hexemer, E. J. Kramer, S. Krishnan, P. M. Petroff, D. A. Fischer, *Macromolecules* **2006**, *39*, 2225.
- [24] M. C. Gather, D. D. C. Bradley, *Adv. Funct. Mater.* **2007**, *17*, 479.
- [25] T. Fujiwara, J. Locklin, Z. N. Bao, *Appl. Phys. Lett.* **2007**, *90*, 232108.
- [26] L. Bürgi, T. J. Richards, R. H. Friend, H. Sirringhaus, *J. Appl. Phys.* **2003**, *94*, 6129.
- [27] H. Sirringhaus, P. J. Brown, R. H. Friend, M. M. Nielsen, K. Bechgaard, B. M. W. Langeveld-Voss, A. J. H. Spiering, R. A. J. Janssen, E. W. Meijer, P. Herwig, D. M. de Leeuw, *Nature* **1999**, *401*, 685.
- [28] D. H. Kim, Y. D. Park, Y. S. Jang, H. C. Yang, Y. H. Kim, J. I. Han, D. G. Moon, S. J. Park, T. Y. Chang, C. W. Chang, M. K. Joo, C. Y. Ryu, K. W. Cho, *Adv. Funct. Mater.* **2005**, *15*, 77.
- [29] M. S. A. Addou, F. P. Orfino, Y. K. Son, S. Holdcroft, *J. Am. Chem. Soc.* **1997**, *119*, 4518.
- [30] I. McCulloch, M. Heeney, C. Bailey, K. Genevicius, I. MacDonald, M. Shkunov, D. Sparrowe, S. Tierney, R. Wagner, W. M. Zhang, M. L. Chabinyc, R. J. Kline, M. D. McGehee, M. F. Toney, *Nat. Mater.* **2006**, *5*, 328.
- [31] Y. H. Geng, A. Trajkovska, D. Katsis, J. J. Ou, S. W. Culligan, S. H. Chen, *J. Am. Chem. Soc.* **2002**, *124*, 8337.
- [32] Y. H. Geng, S. W. Culligan, A. Trajkovska, J. U. Wallace, S. H. Chen, *Chem. Mater.* **2003**, *15*, 542.
- [33] Y. H. Geng, A. C.-A. Chen, J. J. Ou, S. H. Chen, K. Klubek, K. Vaeth, C. W. Tang, *Chem. Mater.* **2003**, *15*, 4352.
- [34] S. W. Culligan, Y. H. Geng, S. H. Chen, K. Klubek, K. Vaeth, C. W. Tang, *Adv. Mater.* **2003**, *15*, 1176.
- [35] A. C.-A. Chen, S. W. Culligan, Y. H. Geng, S. H. Chen, K. Klubek, K. Vaeth, C. W. Tang, *Adv. Mater.* **2004**, *16*, 783.
- [36] J. H. Jo, C. Y. Chi, S. Höger, G. Wegner, D. Y. Yoon, *Chem. Eur. J.* **2004**, *10*, 2681.
- [37] M. P. Aldred, A. E. A. Contoret, S. R. Farrar, S. M. Kelly, D. Mathieson, M. O'Neill, W. C. Tsoi, P. Vlachos, *Adv. Mater.* **2005**, *17*, 1368.
- [38] T. Yasuda, K. Fujita, T. Tsutsui, Y. H. Geng, S. W. Culligan, S. H. Chen, *Chem. Mater.* **2005**, *17*, 264.
- [39] L.-Y. Chen, T.-H. Ke, C.-C. Wu, T.-C. Chao, K.-T. Wong, C.-C. Chang, *Appl. Phys. Lett.* **2007**, *91*, 163509.
- [40] A. Liedtke, M. O'Neill, A. Wertmüller, S. P. Kitney, S. M. Kelly, *Chem. Mater.* **2008**, *20*, 3579.
- [41] H. Thiem, P. Shtrohriegel, S. Setayesh, D. de Leeuw, *Synth. Met.* **2006**, *156*, 582.
- [42] F. Jaramillo-Isaza, M. L. Turner, *J. Mater. Chem.* **2006**, *16*, 83.
- [43] X. J. Zhang, Y. Qu, L. J. Bu, H. K. Tian, J. P. Zhang, L. X. Wang, Y. H. Geng, F. S. Wang, *Chem. Eur. J.* **2007**, *13*, 6238.
- [44] J.-S. Yang, J.-L. Yan, C.-Y. Hwang, S.-Y. Chiou, K.-L. Liao, H.-H. G. Tsai, G.-H. Lee, S.-M. Peng, *J. Am. Chem. Soc.* **2006**, *128*, 14109.
- [45] B. W. D'Andrade, S. Datta, S. R. Forrest, P. Djurovich, E. Polikarpov, M. E. Thompson, *Org. Electron.* **2005**, *6*, 11.
- [46] R. Schueppel, K. Schmidt, C. Uhrich, K. Schulze, D. Wynands, J. L. Brédas, E. Brier, E. Reinold, H.-B. Bu, P. Baeuerle, B. Maennig, M. Pfeiffer, K. Leo, *Phys. Rev. B.* **2008**, *77*, 085311.
- [47] C. D. Dimitrakopoulos, P. R. L. Malenfant, *Adv. Mater.* **2002**, *14*, 99.
- [48] R. C. Weast, *CRC Handbook of Chemistry and Physics*, 64th Edn., CRC Press, FL **1983**, p. F-39.
- [49] J. C. Conboy, E. J. C. Olson, D. M. Adams, J. Kerimo, A. Zaban, B. A. Gregg, P. F. Barbara, *J. Phys. Chem. B* **1998**, *102*, 4516.
- [50] G. Li, V. Shrotriya, J. S. Huang, Y. Yao, T. Moriarty, K. Emery, Y. Yang, *Nat. Mater.* **2005**, *4*, 864.
- [51] Y. Zhao, Z. Y. Xie, Y. Qu, Y. H. Geng, L. X. Wang, *Appl. Phys. Lett.* **2007**, *90*, 043504.
- [52] M. T. Tloyd, A. C. Mayer, S. Subramanian, D. A. Mourey, D. J. Herman, A. V. Bapat, J. E. Anthony, G. G. Malliaras, *J. Am. Chem. Soc.* **2007**, *129*, 9144.
- [53] S. Miller, G. Fanchini, Y.-Y. Lin, C. Li, C.-W. Chen, W.-F. Su, M. Chhowalla, *J. Mater. Chem.* **2008**, *18*, 306.
- [54] F.-C. Chen, H.-C. Tseng, C.-J. Ko, *Appl. Phys. Lett.* **2008**, *92*, 103316.
- [55] K. C. Dickey, J. E. Anthony, Y.-L. Loo, *Adv. Mater.* **2006**, *18*, 1721.
- [56] R. R. Gagné, C. A. Koval, G. C. Lisensky, *Inorg. Chem.* **1980**, *19*, 2854.
- [57] T. Yasuda, K. Fujita, H. Nakashima, T. Tsutsui, *Jpn. J. Appl. Phys. Part 1* **2003**, *42*, 6614.